Int. J. Electrochem. Sci., 12 **(2017)** 2400 – 2411, doi: 10.20964/2017.03.23

International Journal of
ELECTROCHEMICAL
SCIENCE
www.electrochemsci.org

Influence of Y_2O_3/Nd_2O_3 Particles Additive on the Corrosion Resistance of MAO Coating on AZ91D Magnesium Alloy

Jingmao Zhao[1,2], *Kening Ouyang*[1], *Xiong Xie*[1], *Jianwen Zhang*[3,*]

[1] College of Materials Science and Engineering, Beijing University of Chemical Technology, Beijing 100029, China
[2] State Key Laboratory of Materials Electrochemical Process and Technology, Beijing University of Chemical Technology, Beijing 100029, China
[3]College of Chemical Engineering, Beijing University of Chemical Technology, Beijing 100029, China
[*]E-mail: zhangjw@mail.buct.edu.cn

Received: 28 November 2016 / *Accepted:* 4 January 2017 / *Published:* 12 February 2017

Micro-arc oxidation (MAO) coatings with the addition of Y_2O_3/Nd_2O_3 particles were formed on AZ91D magnesium alloy. The corrosion behaviors of the coated AZ91D samples were studied by using potentiodynamic polarization, electrochemical impedance spectroscopy (EIS), and immersion test. Scanning electron microscope (SEM) and energy dispersive spectrometer (EDS) were used to characterize the microstructure and elemental compositions of the coatings. It is found that the micro-pores and defects of the coating decreases with the addition of Y_2O_3 particles, resulting in the improved corrosion resistance, while the corrosion resistance of AZ91D magnesium alloy is decreased with the addition of Nd_2O_3 particles.

Keywords: Magnesium alloy; MAO; Y_2O_3; Nd_2O_3; Corrosion resistance

1. INTRODUCTION

Magnesium alloys have shown promising application in automobiles, aerospace industry and 3C electronics due to the low density, high strength to weight ratio, good electromagnetic shielding property and a high recovery rate[1]. However, the poor corrosion resistance limits their widespread application [2]. Proper surface treatments involving chemical conversion, anodization, sol–gel, organic and metallic coating can improve the corrosion resistance of magnesium alloy [3].

Micro-arc oxidation (MAO) is an attractive surface engineering technique for some metals such as aluminum, magnesium, titanium, and zirconium. In an electrolytic bath with high external voltages (400–600 V), the metal surface can be converted into a dense and hard ceramic oxide coating. Due to

its simplified pre-treatment, superior corrosion and wear resistance performance and environmentally safe coating process, MAO technology has emerged as an important alternative to anodizing techniques in certain areas [4]. Recently, most of the researches on MAO coating formed on magnesium alloy have been focused on electrolyte components [5-6] and process parameters such as pulse frequency, oxidation time, electrolyte concentration, and applied voltage [7-9]. According to the research results, the chemical stability and mechanical properties of the coating can be improved with the addition of nano-particles such as titanium oxide (TiO_2), zirconium dioxide (ZrO_2), and graphite [10-12]. However, the influence of rare earth oxide particles on the corrosion resistance of MAO coating has rarely studies. Zhu et al [13] studied the microstructure and properties of the low-power-laser clad coatings on magnesium with different amount of Y_2O_3 addition. It was found that the micro-hardness, abrasion and corrosion resistance of the coatings were greatly improved compared with the magnesium matrix, especially for Al-Cu coating with Y_2O_3 addition. Chen et al [14] found that the surface quality of MAO coating on AZ31D magnesium alloy was improved by the addition of $Nd(NO_3)_3$ in the phosphate system electrolyte, which attributed to the formation of Nd_2O_3 and $Nd(OH)_3$ in the coatings. To further enhance the anti-corrosion performance of MAO coating, Y_2O_3 and Nd_2O_3 particles are chosen to be added into the electrolyte, and the surface morphology and corrosion resistance of MAO coating on AZ91D magnesium alloy were investigated in this work.

2. EXPERIMENTAL

2.1 Sample preparation

Samples with the size of 35mm×35mm×2mm made from an AZ91D magnesium alloy, whose compositions were listed in Table1, were used as the substrate in this investigation. The samples were abraded with silicon carbide abrasive paper up to 1000 grit and washed with deionized water, ethanol and acetone to avoid any surface contamination and then dried for later use.

Table 1. The compositions (wt.%) of AZ91D magnesium alloy

Al	Zn	Mn	Si	Cu	Ni	Fe	Mg
9.4	0.82	0.23	0.01	0.02	0.002	0.005	Remainder

MAO was performed using MAD-20 power (Chengdu PULSETECH Electrical Co., LTD China). The untreated AZ91D substrate was denoted as sample “S”. The sample developed in the base electrolyte (25g/L $Na_2SiO_3.9H_2O$ + 20g/L KOH + 5g/L $KF{\cdot}2H_2O$ + 5g/L $C_6H_5Na_3O_7{\cdot}2H_2O$ + 10mL/L $C_3H_8O_3$， pH=14) was denoted as sample “B”. Sample “Y” and “N” developed in the base electrolyte with 5g/L Y_2O_3 particles(208nm) and 5g/L Nd_2O_3 particles(390nm) respectively. Ultrasonic and mechanical stirring were employed to prevent the particles from deposition during MAO process. Analytical reagents and distilled water were used to prepare the electrolytes.

MAO electrical parameters were set as follows: the current density was 50mA/cm^2, the duty cycle was 10%, the frequency was 300Hz, and the temperature of electrolytes was controlled to stay between 20 and 30^{o}C by using water-cooling system.

2.2 Characterization of coatings

To evaluate the corrosion resistance of MAO coatings, potentiodynamic polarization and electrochemical impedance spectroscopy (EIS) were performed for the substrate and MAO treated Mg samples using PARSTAT2273. All the polarization and EIS tests were carried out at room temperature in 3.5 wt.% NaCl solution with a pH of 6.5. A conventional three-electrode cell was used with a platinum electrode as auxiliary electrode and a saturated calomel electrode as the reference electrode respectively. Untreated and MAO treated Mg samples were used as working electrodes, exposing 1.0 cm^2 of area to the solution during the electrochemical measurements. The potentiodynamic polarization was performed with a scan rate of 1mV·s^{-1} and a scan voltage range of -0.4~0.4V vs. open circuit potential (OCP). Electrochemical impedance spectroscopy (EIS) was conducted at OCP with an ac amplitude of 10 mV(peak-to-peak) in the frequency range from 100 kHz to 0.01Hz. Before each measurement, the working electrode was immersed in the solution at least for 30 minutes to reach a stable state (the OCP fluctuation was less than ±5 mV). Three measurements were performed for each experimental condition to estimate the repeatability, with a relative standard deviation of less than 10%.

The corrosion resistance of MAO coatings was also examined by immersion test. PVC tubes with 25 mm in diameter and 50mm in height were put on the Mg samples (treated and untreated) and fixed by silicon rubber. Then 20 ml of 3.5 wt.% NaCl solution was put in the tube. The surface of samples exposed to the solution was observed by a digital camera after immersion of 4h, 96h and 216h respectively.

Malvern Zetasizer was employed to measure the zeta-potential of the Y_2O_3 and Nd_2O_3 particles in the base electrolyte. SEM and EDS were used to observe the surface morphology and analyze the compositions of the surface and cross-section of the samples. The thickness of MAO coatings was measured by a digital thickness gauge. Twenty points were measured at each sample randomly. The average value was calculated and used to represent the coating thickness of the sample.

3. RESULTS AND DISCUSSION

3.1 Potentiodynamic polarization curve measurements

The potentiodynamic polarization curves of AZ91D samples(S, B, N and Y) in 3.5wt.% NaCl solution are shown in Fig. 1. It can be seen that all the polarization curves of AZ91D samples treated with MAO are shifted to the left direction (lower current density direction) and the corrosion resistances of AZ 91D are remarkably enhanced by MAO treatment.

The polarization curves were fitted by using Cview software, and the fitted values of the cathodic Tafel slope (*Bc*), anodic Tafel slope (*Ba*), corrosion potential (E_0) and corrosion current

density (I_o) are listed in Table 2. Compared to sample S, the corrosion potential of sample B decreases slightly from -1.5471V to -1.5645V and the corrosion current density decreases two orders of magnitude. With the addition of Y_2O_3 particles to the base electrolyte, the corrosion potential increases from -1.5645V (sample B) to -1.3911V (sample Y) and the corrosion current density further decreases from 1.2×10^{-7} A.cm^{-2} to 5.3×10^{-8} A.cm^{-2}. However, the corrosion current density increases to 8.7×10^{-7} A.cm^{-2} with addition of Nd_2O_3 particles. Therefore, the corrosion resistance of MAO coating is enhanced by adding Y_2O_3, which is agreement with the results of Zhu et al [13], and decreased by adding Nd_2O_3.

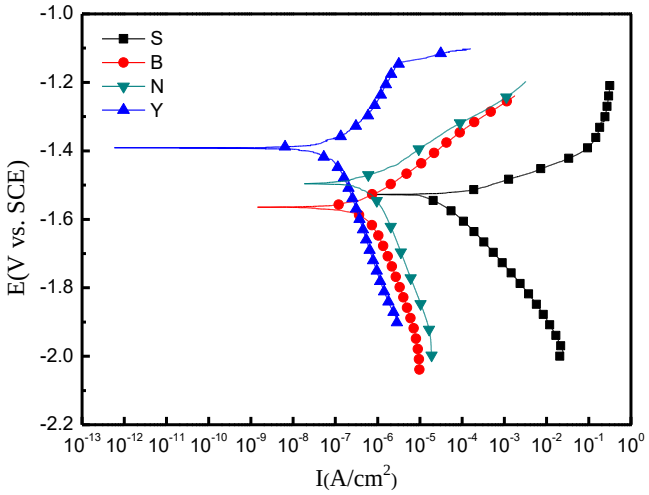

Figure 1. Polarization curves of MAO coatings in 3.5wt.% NaCl solution (S: AZ91D; B: AZ91D treated by MAO in the base electrolyte; Y: AZ91D treated by MAO in the base electrolyte with 5g/L Y_2O_3 particles; N: AZ91D treated by MAO in the base electrolyte with 5g/L Nd_2O_3 particles)

Table 2. Electrochemical parameters obtained from polarization curves of MAO coatings in 3.5wt.% NaCl solution(S: AZ91D; B: AZ91D treated by MAO in the base electrolyte; Y: AZ91D treated by MAO in the base electrolyte with 5g/L Y_2O_3 particles; N: AZ91D treated by MAO in the base electrolyte with 5g/L Nd_2O_3 particles)

Sample	E_0(V.vs.SCE)	Ba(mV.dec^{-1})	Bc(mV.dec^{-1})	I_0(A.cm^{-2})
S	-1.5471	34.6	-144.5	3.7×10^{-5}
B	-1.5645	47.3	-76.9	1.2×10^{-7}
Y	-1.3911	79.1	-152.4	5.3×10^{-8}
N	-1.4954	106.9	-299.0	8.7×10^{-7}

3.2 EIS measurements

Fig. 2 shows the EIS plots of untreated and MAO treated AZ91D magnesium alloy in 3.5wt.% NaCl solution respectively. The Bode spectrums for sample B, N and Y have two time-constants, one is related to the outer pore layer and the other to the inner barrier layer of MAO coating. As shown in

Fig.2, the corrosion resistance of AZ91D magnesium alloy can be improved greatly by MAO treatment, and an increase in the semicircle's diameter is observed for sample Y and decrease for sample N compared to sample B, indicating that the addition of Y_2O_3 can enhance the corrosion resistance of MAO coating, while Nd_2O_3 additive shows the negative effect. This result is in good agreement with that obtained from the polarization curves.

Fig. 3 presents the two equivalent circuits which best fit the experimental data. In Fig. 3(a), R_s, CPE, and R_{ct} present the solution resistance offered by corrosive electrolyte, constant phase element and charge transfer resistance respectively. In Fig.3(b), R_s, R_{po}, R_b represent the solution resistance, pore resistance and barrier layer resistance, respectively. CPE_{po} and CPE_b refer to the constant phase elements corresponding to pore and inner barrier layer.

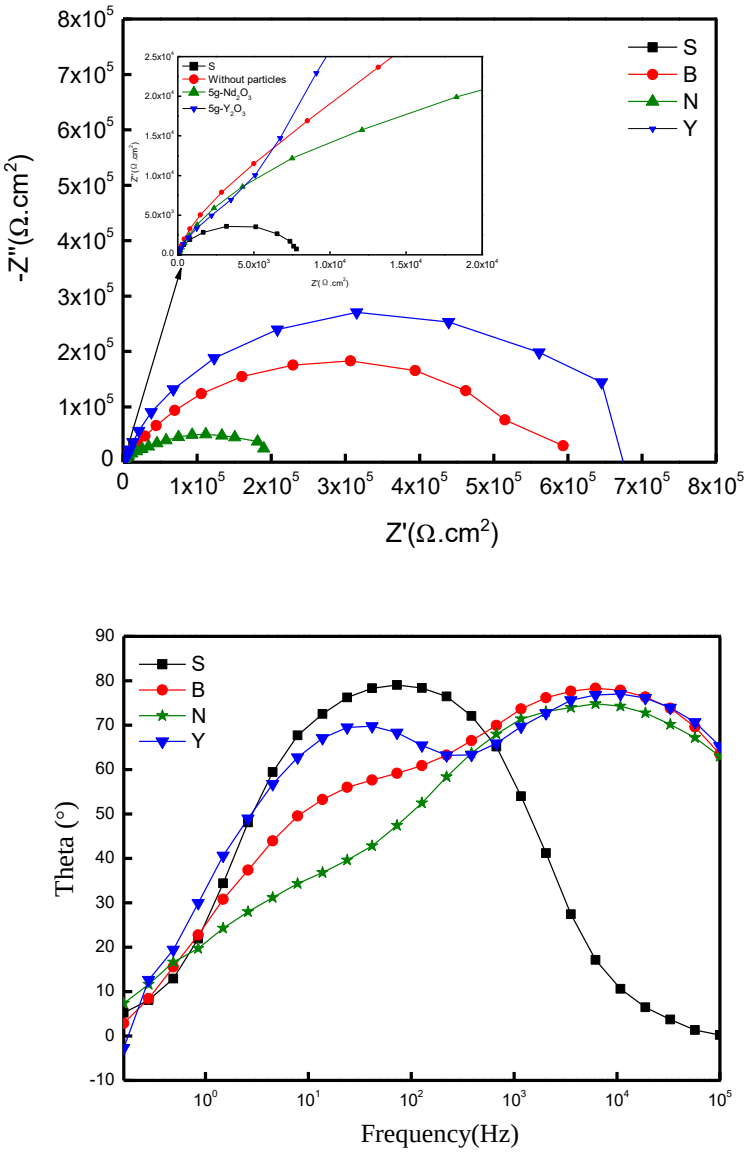

Figure 2. Nyquist plots and Bode plots of MAO coatings in 3.5wt.% NaCl solution (S: AZ91D; B: AZ91D treated by MAO in the base electrolyte; Y: AZ91D treated by MAO in the base electrolyte with 5g/L Y_2O_3 particles; N: AZ91D treated by MAO in the base electrolyte with 5g/L Nd_2O_3 particles)

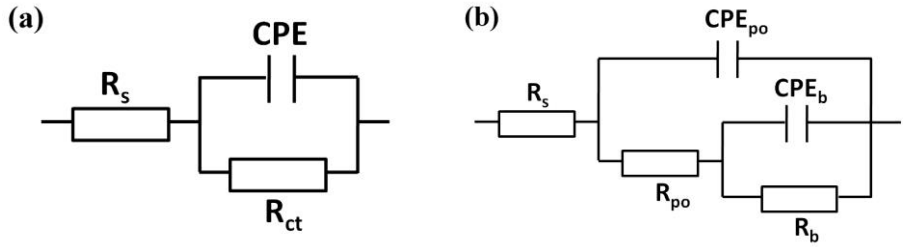

Figure 3. Equivalent circuits used to fit the EIS plots of MAO coatings

The EIS plots were fitted by using Zsimpwin software and the results are shown in Table 3. From which we can see that the corrosion resistance of AZ91D magnesium alloy can be improved greatly by MAO treatment, and CPE_{po} or CPE_b decreases and R_{po} or R_b increases by the addition of Y_2O_3 when compare the EIS data of sample Y with sample B. The lower CPE value means the lower film porosity and thereby better corrosion resistance of MAO coating [15]. This is consistent with the polarization curve and EIS results. However, addition of Nd_2O_3 shows little effect on the corrosion resistance of MAO. It also can be seen from Table 3 that R_b is almost ten times larger than R_{po}, therefore the corrosion resistance of the MAO coating is mainly dependent on the inner barrier layer.

Table 3. Electrochemical parameters obtained from EIS plots of MAO coatings in 3.5wt.% NaCl solution(S: AZ91D; B: AZ91D treated by MAO in the base electrolyte; Y: AZ91D treated by MAO in the base electrolyte with 5g/L Y_2O_3 particles; N: AZ91D treated by MAO in the base electrolyte with 5g/L Nd_2O_3 particles)

Sample	CPE ($F.cm^{-2}$)	CPE_{po} ($F.cm^{-2}$)	n_1	R_{ct} ($\Omega.cm^2$)	R_{po} ($\Omega.cm^2$)	CPE_b ($F.cm^{-2}$)	n_2	R_b ($\Omega.cm^2$)
S	1.13×10^{-5}	--	0.93	7.9×10^{3}	--	--	--	--
B	--	6.38×10^{-8}	0.90	--	3.8×10^{4}	2.68×10^{-7}	0.69	5.5×10^{5}
Y	--	1.15×10^{-8}	0.88	--	4.0×10^{5}	2.62×10^{-8}	0.78	4.2×10^{6}
N	--	1.19×10^{-7}	0.85		3.6×10^{4}	1.49×10^{-6}	0.59	1.8×10^{5}

3.3 Immersion test

Localized corrosion is the main corrosion form of MAO coated magnesium alloy in Cl^--containing solution [16], so the effect of Y_2O_3 and Nd_2O_3 addition on localized corrosion of MAO coating was evaluated via an immersion test in 3.5wt.% NaCl solution at room temperature. The macro-appearances of the corroded samples at different immersion times are shown in Fig.4. After 96 h immersion, sample S suffers serious corrosion with large pits on the surface, sample N suffers relatively slight corrosion with a few pits, while sample B and Y remain undamaged. As the immersion time extends to 216h, the corrosion of sample S becomes more severely, a great deal of corrosion products, mainly composed of $Mg(OH)_2$ and $Mg_2(OH)_3Cl{\cdot}5H_2O$ [17], fall off from the alloy surface. One pit is found on the surface of sample B and many pits appear on the surface of sample N. However,

sample Y is not damaged at all. Therefore, the resistance of the MAO coatings to localized corrosion is enhanced by the addition of Y_2O_3 particles.

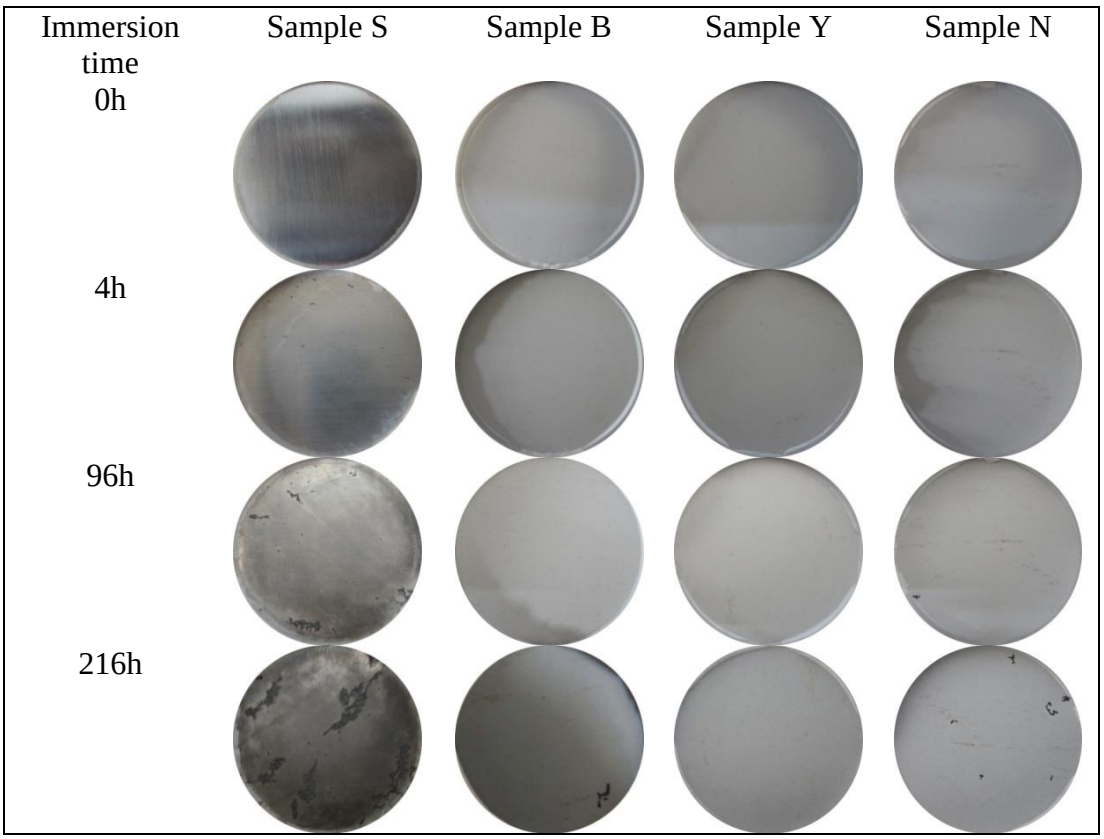

Figure 4. Surface morphologies of the untreated and MAO treated AZ91 Mg alloys immersed in 3.5wt.%NaCl solution for different time (S: AZ91D; B: AZ91D treated by MAO in the base electrolyte; Y: AZ91D treated by MAO in the base electrolyte with 5g/L Y_2O_3 particles; N: AZ91D treated by MAO in the base electrolyte with 5g/L Nd_2O_3 particles)

3.4 The thickness of MAO coatings

Table 4 lists the average thickness of MAO coatings of sample B, sample Y and sample N. It can be seen from Table 4 that the addition of Y_2O_3 and Nd_2O_3 has little influence on the thickness of the coating. The thickness of the MAO coating is mainly dependent upon the oxidation time and electrolyte composition [18-19].

Table 4. The average thickness of MAO coatings(B: AZ91D treated by MAO in the base electrolyte; Y: AZ91D treated by MAO in the base electrolyte with 5g/L Y_2O_3 particles; N: AZ91D treated by MAO in the base electrolyte with 5g/L Nd_2O_3 particles)

Sample	B	Y	N
Thickness	19.8μm	20.1μm	19.5μm

3.5 The voltage versus time curve

The time-transient behaviors of the voltage response of the AZ91D Mg alloy processed in electrolytes with and without Y_2O_3/Nd_2O_3 particles by applying a current density of 50 mA/cm^2 are represented in Figure 5. The MAO process can be divided into three stages in the voltage-time curve: general anodization, micro-arc oxidation and arc oxidation [20]. In the first 60 seconds (stage1), a very thin and insulated ceramic coating is formed on the surface of Mg alloy under anodic current via the reaction between substrate and electrolyte, the voltage increases rapidly to around 250V, the addition of Y_2O_3 or Nd_2O_3 particles has little influence at this stage. As time prolongs (stage 2), light sparks occur on the coating surface and the color of sparks turns from white to orange, a dense layer of the MAO coating is formed at this stage. The measured zeta-potentials of Nd_2O_3 and Y_2O_3 particles are -15.7mV and -18.2mV in the base electrolyte respectively. This indicates that Y_2O_3 and Nd_2O_3 particles are negative charged, so they will migrate to the anode surface under the effect of electrophoresis and involve in the formation of coating. After the voltage exceeds 300V (stage 3), the voltage increasing tendency becomes slower, a mass of loose MgO and Mg_2SiO_4 phase are quickly produced at this stage, which is mainly responsible for the thickening of coatings. It can be seen that the potential values of sample Y is higher than that of sample B, this may be attributed to a more dense MAO coating formed on sample Y, while the effect of Nd_2O_3 is the opposite. This result is consistence with the corrosion resistance of the coating with Y_2O_3 and Nd_2O_3 particles.

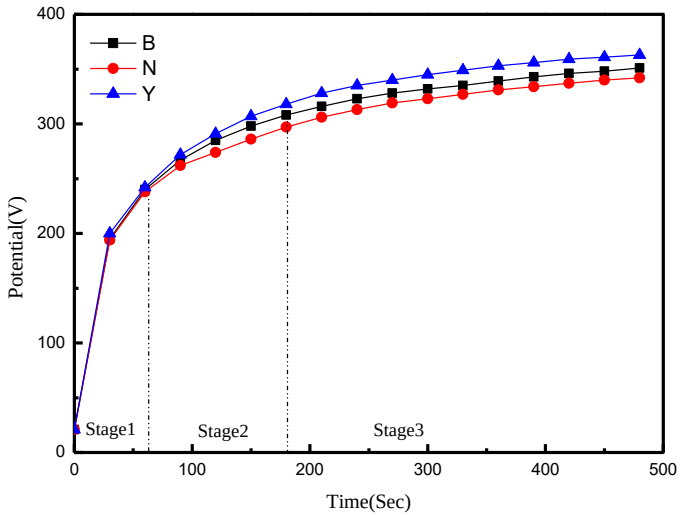

Figure 5. Variation of voltage responses during the MAO process (B: AZ91D treated by MAO in the base electrolyte. Y: AZ91D treated by MAO in the base electrolyte with 5g/L Y_2O_3 particles; N: AZ91D treated by MAO in the base electrolyte with 5g/L Nd_2O_3 particles)

3.6 Surface and cross section morphologies of MAO coating

Fig.6 presents the surface and cross-sectional morphologies of sample B, N and Y. EDS analysis results of sample B, N and Y are listed in Table 5. Element Nd and Y are present in the surface of sample N and Y, which means that Y_2O_3 or Nd_2O_3 particles have incorporated into the

coating during MAO process. Fig.7 and Fig. 8 show the elemental mapping in the cross section of N and Y samples respectively. It is also proved that the Y_2O_3 and Nd_2O_3 particles have been doped in the coatings. By Adobe Photoshop CS software, the percentage area of porosity of MAO coatings can be calculated and the results are listed in Table 6. As shown in Table 6, the percentage area of porosity of MAO coating decreases with the addition of Y_2O_3, but increases slightly with the addition of Nd_2O_3. Figure 6 shows that many micro-pores and defects exist on the cross-section of sample B and N, while a more compact MAO coating with small amount of micro-pores and defects is formed on the surface of sample Y, thereby enhancing its corrosion resistance. Lee et al. [21] have evaluated the plasma temperature during plasma oxidation processing of AZ91Mg alloy through analysis of the melting behavior of incorporated particles. They assumed that the temperature of the arc plasma is in the range of 2116–2643 K. The melting points of Y_2O_3 and Nd_2O_3 are 2683K and 2173K, respectively; therefore, Nd_2O_3 can be melted or transformed to a new oxide phase, while Y_2O_3 cannot be melted during MAO process and still present in the coating in solid particles. They can seal the micropores of MAO coating and decrease the film porosity. This fact may be the reason why Y_2O_3 can enhance the anti-corrosion performance of MAO coating and Nd_2O_3 cannot. There might be a physical effect of blocking pores for Y_2O_3 particles, and also there might be a chemical effect caused by inhibition, and the detailed mechanism should be further investigated.

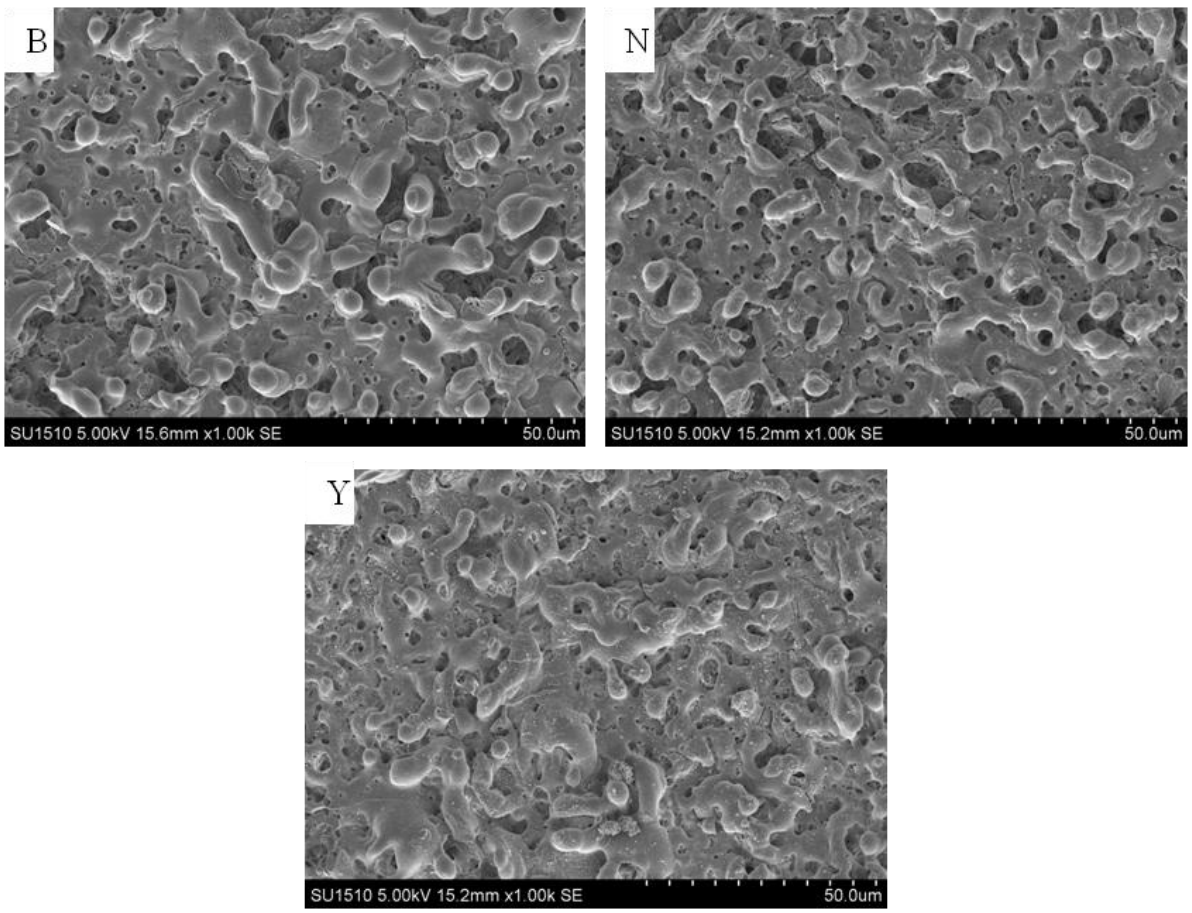

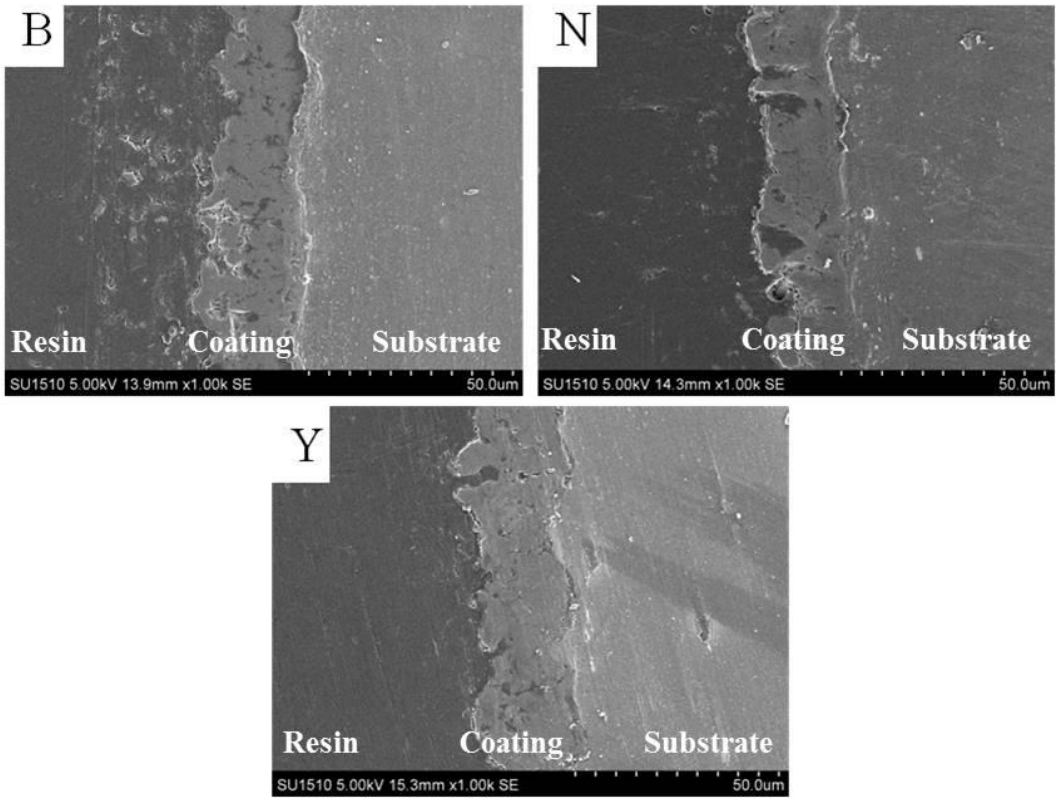

Figure 6. Surface and cross-sectional morphologies of MAO coatings (B: AZ91D treated by MAO in the base electrolyte; N: AZ91D treated by MAO in the base electrolyte with 5g/L Nd_2O_3 particles; Y: AZ91D treated by MAO in the base electrolyte with 5g/L Y_2O_3 particles)

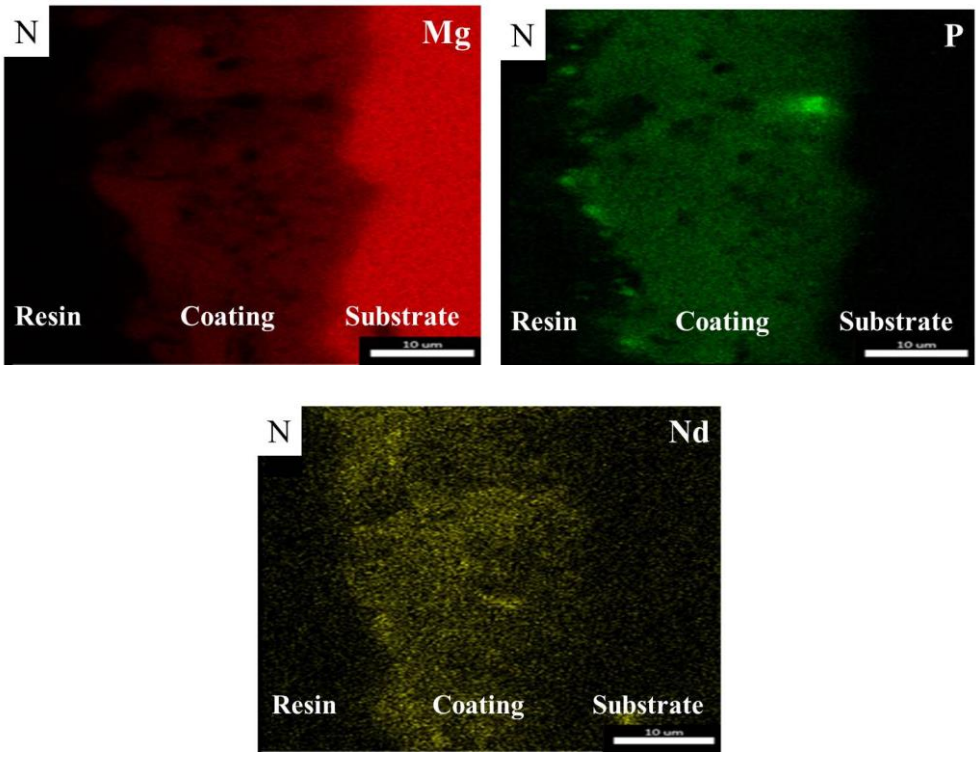

Figure 7. Elemental mapping of MAO coating **(**AZ91D treated by MAO in the base electrolyte with 5g/L Nd_2O_3 particles)

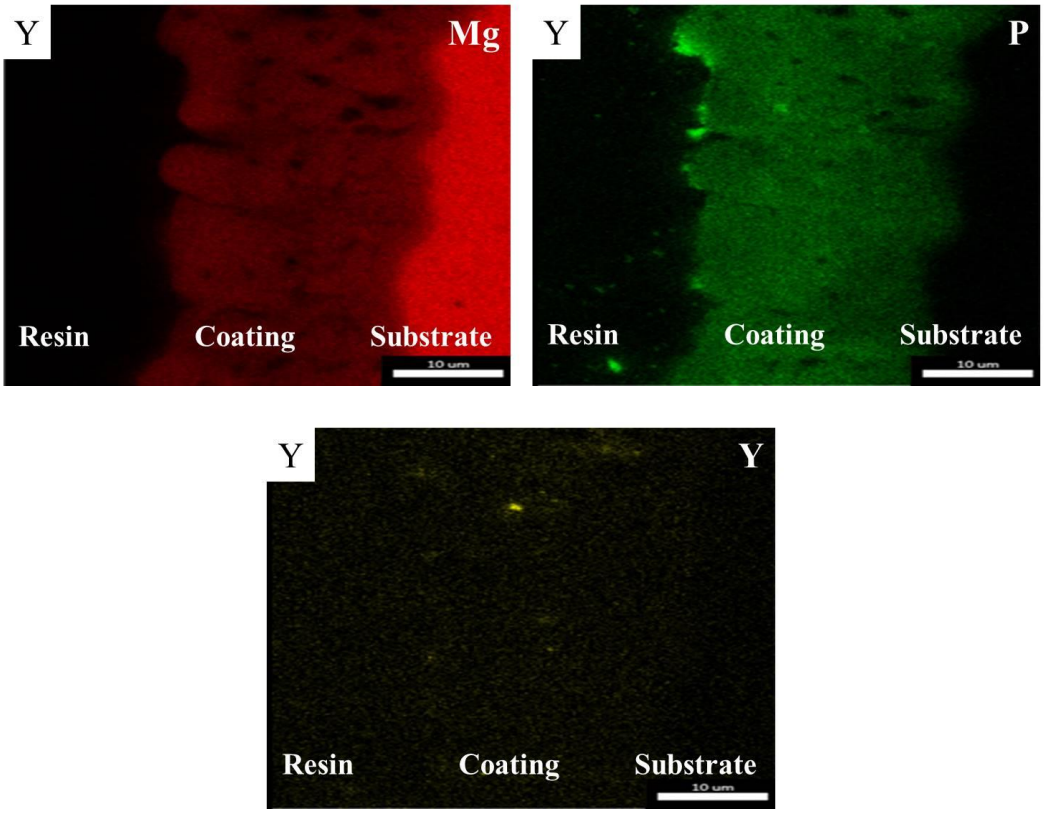

Figure 8. Elemental mapping of MAO coating (AZ91D treated by MAO in the base electrolyte with 5g/L Y_2O_3 particles)

Table 5 Elemental contents (at.%) of MAO coating surface (B: AZ91D treated by MAO in the base electrolyte; N: AZ91D treated by MAO in the base electrolyte with 5g/L Nd_2O_3 particles; Y: AZ91D treated by MAO in the base electrolyte with 5g/L Y_2O_3 particles)

Sample	O	Mg	Si	Al	F	Nd	Y
B	34.66	52.15	10.14	2.46	0.58		
N	56.26	30.39	5.69	2.62	1.71	3.34	
Y	58.86	23.33	12.83	1.54	0.95		2.49

Table 6. Percentage area of porosity of MAO coating surface (B: AZ91D treated by MAO in the base electrolyte; N: AZ91D treated by MAO in the base electrolyte with 5g/L Nd_2O_3 particles; Y: AZ91D treated by MAO in the base electrolyte with 5g/L Y_2O_3 particles)

Sample	B	N	Y
Area of porosity(%)	12.1	14.9	7.5

4. CONCLUSIONS

(1) Adding Y_2O_3 particles can decrease the porosity of MAO coating on AZ91D substrate, but has little effect on the thickness of the coating.

(2) Corrosion resistance of AZ91D alloy can be obviously enhanced by adding Y_2O_3 particles into the electrolyte during the MAO process.

(3) Adding Nd_2O_3 particles to the MAO coating can decrease the corrosion resistance of magnesium alloy.

ACKNOWLEDGEMENTS
The authors acknowledge the National Key Technology R&D Program of China (2015BAK39B00) for supporting this work.

References

1. B. L. Mordike, T. Ebret, *Mater. Sci. Eng*., A, 302 (2001) 37
2. G. L. Song, A. Atrens, *Adv. Eng. Mater*. 1 (1999) 11
3. J.E. Gray, B. Luan, *J. Alloys Compd*. 336 (2002) 88
4. G.L. Song ,Corrosion Prevention of Magnesium Alloys, Woodhead Publishing Limited, 2013, Pages 163
5. D. Sreekanth, N. Rameshbabu and K. Venkateswarlu, Ceramics international, 38 (2012) 4607
6. Ghasemi, V. S. Raja and C. Blawert, *Surf. Coat. Technol*., 104 (2010) 1469
7. I.J. Hwang,D.Y. Hwang and Y.G. Ko, *Surf. Coat. Technol*., 206 (2012) 3360
8. S.V. Gnedenkov, O.A. Khrisanfova and A.G. Zavidnaya, *Surf. Coat. Technol*., 204 (2010) 2316
9. B. M. Wilke, L. Zhang, W.P. Li, C.Y. Ning, C.F. Chen,Y.H. Gu, *Appl. Surf. Sci*.,363(2016)328
10. T. S. Lim, H. S. Ryu and S. H. Hong, *Corros. Sci*., 62 (2012) 104
11. K. M. Lee, K. R. Shin and S. Namgung, *Surf. Coat. Technol*., 205 (2011) 3779
12. G. H. Lv, H. Chen and W. C. Gu, *Curr. Appl. Phys*. 9 (2009) 324
13. R. Zhu, Z. Y. Li and X. X. Li, *Appl. Surf. Sci*., 353 (2015) 405
14. B. T. Chen, P. F. Li and F. Guo, *Surf. Technol*., 38 (2009) 20 (Chinese)
15. D. Sreekanth, N. Rameshbabu and K. Venkateswarlu, *Ceram. Int*. 38 (2012) 4607
16. H. X. Guo, Y. Ma and J. S. Wang, *Transactions of Nonferrous Metals Society of China*, 22 (2012) 1786
17. L.Q. Bai, K.Y. Shu and D. Li, *Journal of Aeronautical Materials*, 30 (2010) 32 (Chinese)
18. S. Durdu, S. Bayramoğlu and A. Demirtaş, *Vacuum*, 88 (2013) 130
19. J.M. Li, B.L. Jing and X.T. Jing, *Transactions of Materials and Heat Treatment*, 24 (2003) 63 (Chinese)
20. L. Chang, *J. Alloys Compd*., 468 (2009) 462
21. K. M.Lee, B. U. Lee, S. Il Yoon, E. S. Lee, B. Yoo, D. H. Shin, *Electrochimica Acta*, 67 (2012) 6